VII International Conference on Computational Methods for Coupled Problems in Science and Engineering
COUPLED PROBLEMS 2017
M. Papadrakakis, E. Oñate and B. Schrefler (Eds)

A COMPARATIVE STUDY OF INTERFACE CAPTURING METHODS WITH AMR FOR INCOMPRESSIBLE TWO-PHASE FLOWS

OSCAR ANTEPARA[*†], NESTOR BALCAZAR[*] AND ASSENSI OLIVA[†]

[*]Termo Fluids S.L.
Avda Jacquard 97 1-E, 08222 Terrassa (Barcelona), Spain
e-mail: termofluids@termofluids.com, web page: http://www.termofluids.com/

[†]Heat and Mass Transfer Technological Center (CTTC)
Universitat Politécnica de Catalunya-BarcelonaTech (UPC)
ETSEIAAT, Colom 11, 08222 Terrassa, Barcelona, Spain
e-mail: cttc@upc.edu, web page: http://www.cttc.upc.edu

Key words: Adaptive Mesh Refinement, interface capturing methods, two phase flows

Abstract. This paper presents a comparative study of interface capturing methods with adaptive mesh refinement for Direct Numerical Simulation (DNS) of incompressible two-phase flows. The numerical algorithms for fluid motion and interface capturing methods have been previously introduced in the context of the finite-volume approach for both mass conservative level-set methodology and coupled volume-of-fluid/level-set method for unstructured/structured fixed meshes. The Adaptive Mesh Refinement (AMR) method introduced in consist on a cell-based refinement technique to minimize the number of computational cells and provide the spatial resolution required for the interface capturing methods. The present AMR framework adapts the mesh according to a physics-based refinement criteria defined by the movement of the interface between the fluid-phases. Numerical experiments are presented to evaluate the methods described in this work. This includes a study of the hydrodynamics of single bubbles rising in a quiescent viscous liquid, including its shape, terminal velocity, and wake patterns. These results are validated against experimental and numerical data well established in the scientific literature, as well as a comparison of the different approaches used.

1 INTRODUCTION

Rising bubble in quiescent viscous liquid has become recently in one of the major active research topics in multiphase science. Some computational studies have used detailed simulations of the bubble rising physics in two and three dimensions to explore the fluid effects and its dynamic behavior. In this context, the buoyancy-driven motion of a single

bubble can be used as a well-studied phenomenon to compare and evaluate different interface capturing methods and the use of adaptive mesh refinement algorithm to run dynamic simulations and give a new insight into the utilization of this tool for hexahedral and tetrahedral meshes.

In standard level-set (SLS) methods the interface is defined implicitly by the zero contour of a signed distance function [1]. An advection equation governs the evolution of this function in space and time, combined with a unique re-distancing algorithm. It is established the advantages of this method lies on the accurate computation of interface curvatures and normals, besides the drawback of the appearance of numerical errors that leads to loss or gain of mass. This problem is handled with a conservative level-set (CLS) [11, 6]. A review of the Volume of Fluid(VOF) method can be found in [3, 4]. In this approach, the interface is represented implicitly by a color function, determined to be the fraction of volume in each cell of one of the fluids. The interface needs to be reconstructed using a geometric technique to advect the VOF function[12]. An advantage of VOF method is the fact that certain algorithms can be used to advect the interface so that the mass can be conserved, while still maintaining a sharp representation of the interface. However, a disadvantage of the VOF method is the fact that it is hard to compute correct curvatures from the color function because it presents a step discontinuity at the interface. VOF/LS methods described by many authors [2, 5, 9] results as a combination of both approaches described before, bringing a whole approach for the interface capturing methods. In this way, the interface properties are obtained through a level-set method while mass conservation problems are avoided by using the VOF method.

In this work, the primary motivation is to discuss the simulation of rising bubbles to assess and compare the accuracy of interface capturing methods (CLS and VOF/LS) introduced in our previous works[6, 7, 8, 9, 10]. When using those numerical approaches to solving 2D and 3D multiphase problems, one of the disadvantages is the use of extensive computational resources to address the interfaces of the flows involved entirely. An efficient way to reduce the computational resources, computation time and still be able to have the spatial resolution required is using an adaptive mesh refinement (AMR) method introduced in previous work [13]. Some authors started to use AMR on multiphysics, and multiscale problems to get robust and accurate numerical results for problems, wherein without the use of AMR were much difficult to reach. On the literature, AMR with a Front-Tracking (FT) method was applied to series of rising bubble simulations in the wobbling regime [17]. Also, AMR with a hybrid LS/FT were useful to solve 2D two-phase flows in the presence of surface tension [18].

The outline of the paper is as follows: A summary of the governing equations is given in Section 2. Here, the coupling of the NavierStokes equations for two-phase flow is introduced through the inter-phase conditions, which incorporate surface tension. Moreover, a description of the AMR implementation is shown. The code validation and numerical results are displayed in Section 3. The conclusions are presented in Section 4.

2 MATHEMATICAL MODEL AND NUMERICAL METHODS

2.1 Incompressible two-phase flow

The momentum and mass conservation of two immiscible incompressible and Newtonian fluids are described by the Navier-Stokes equations defined a single fluid in Ω, with a singular source term for the surface tension force at the interface Γ [6, 10, 19, 20, 22]:

$$\frac{\partial}{\partial t}(\rho \mathbf{v}) + \nabla \cdot (\rho \mathbf{v}\mathbf{v}) = -\nabla p + \nabla \cdot \mu \left(\nabla \mathbf{v} + (\nabla \mathbf{v})^T\right) + \rho \mathbf{g} + \sigma \kappa \mathbf{n} \delta_\Gamma \tag{1}$$

$$\nabla \cdot \mathbf{v} = 0 \tag{2}$$

where ρ and μ are the density and dynamic viscosity of the fluids, $\mathbf{g}$ is the gravity acceleration, p is the pressure, $\mathbf{v}$ is the velocity field, the super-index T represents the transpose operator, δ_Γ is a Dirac delta function at the interface Γ, σ is the surface tension coefficient, κ is the curvature of the interface and $\mathbf{n}$ denotes the unit normal vector on the interface. Physical parameters change discontinuously across the interface:

$$\rho = \rho_1 H_1 + \rho_2 (1 - H_1) \qquad \mu = \mu_1 H_1 + \mu_2 (1 - H_1) \tag{3}$$

with ρ_1, ρ_2 and μ_1, μ_2 being the densities and viscosities of the first and second fluids, respectively, whereas H_1 is the Heaviside step function that is one at fluid 1 and zero elsewhere[6, 10].

2.2 Conservative level set equations

In the context of conservative level set (CLS) method[11, 6, 10], a regularized indicator function, ϕ, is employed as follows $\phi(\mathbf{x}, t) = 0.5\,(tanh\,(d(\mathbf{x}, t)/2\varepsilon) + 1)$, where d is a signed distance funtion, $\varepsilon = 0.5h^{0.9}$ is a tunable parameter that sets the thickness of the profile, h is the grid size[6, 10]. With this profile the interface Γ is defined by the location of the $\phi = 0.5$ iso-surface[6, 11], $\Gamma = \{\mathbf{x} \mid \phi(\mathbf{x}, t) = 0.5\}$. Since the level set function is avected by an incompressible velocity field, the following interface transport equation can be written in conservative form:

$$\frac{\partial \phi}{\partial t} + \nabla \cdot \phi \mathbf{v} = 0 \tag{4}$$

The level set function must be reinitialized to keep the profile and thickness of the interface constant following the next equation[6, 11]

$$\frac{\partial \phi}{\partial \tau} + \nabla \cdot \phi(1 - \phi)\mathbf{n} = \nabla \cdot \varepsilon \nabla \phi \tag{5}$$

The reader is referred to [6] for further details on the CLS method on unstructured meshes applied to this work.

2.3 Coupled volume-of-fluid/level-set method

In the volume-of-fluid method[3], an indicator function f is used to track the interface,

$$f(\mathbf{x},t) = \begin{cases} 1 & \text{if } \mathbf{x} \in \Omega_1 \\ 0 & \text{if } \mathbf{x} \in \Omega_2 \end{cases} \tag{6}$$

with Ω_1 and Ω_2 the sub-domains occupied by the fluid 1 and 2 respectively. Discretely, the information stored at the cell Ω_P is the volume-averaged indicator function, namely the volume fraction $f_P = \int_{\Omega_P} f(\mathbf{x},t)dV / \int_{\Omega_P} dV$, where V is the volume of the cell Ω_P. The advection equation for f is given by:

$$\frac{\partial f}{\partial t} + \mathbf{v} \cdot \nabla f = 0 \tag{7}$$

where $\mathbf{v}$ is the fluid velocity. The reader is referred to [12] for further details of the VOF-PLIC method used in the present work. The main idea in the coupled VOF/LS methods [2, 5] is to take the advantages of both approaches (VOF and LS). In the present formulation, the mass losses are reduced through the application of a VOF-PLIC method, while a fine representation of the interface curvature is preserved by utilizing the level set method. From the geometrical data of the interface given by the VOF-PLIC method, a signed distance function is reconstructed following a geometric algorithm[9]. Then, the signed distance function is used to compute surface tension forces. The reader is referred to [9] for further details on the VOF/LS method utilized in the present work.

2.4 Adaptive mesh refinement

Our computational approach uses an adaptive mesh refinement algorithm(AMR) based on a quad/octree for 2D and 3D grids. The reader is referred to [13, 14, 15] for details of the model and the numerical implementation for the use of this methodology to the simulation of turbulent flow around bluff bodies, and [16] for the application of AMR of [13] to the CLS method developed by [6]. The algorithm generates a new mesh according to a physical criterion. The implementation of the AMR algorithm follows the next steps:

Physics-based criterion computation. It is based on the indicator function used to track the interface. On this paper, the cells marked to refinement are the ones with an interface value between 0 and 1. Next, a group of neighbor cells is flagged as well, to ensure a refinement thickness surrounding the interface on both fluids direction. On the moment of one cell of the group does not match the conditions then the subinterval of time is stopped to continue to the next steps. Fig. 1 is an example of the bubble interface and the cells surrounding it to a maximum level.

Creation of the newly adapted meshes. For each AMR time interval, the current mesh, a list of global identifiers of cells, its corresponding level of refinement and, a tree data structure that keeps track of the cells decomposition are processed to create and return the newly mesh.

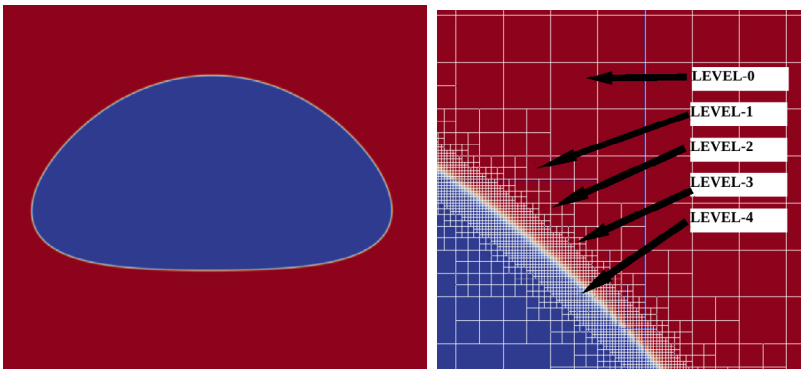

Figure 1: Illustration of refinement process for a two-dimensional rising bubble, where four levels of refinement has been applied.

Solution exchange. The intermediate solutions are transferred from one mesh to the newly. For now, we use a hierarchical cell evaluation mechanism: given any cell in the domain, it provides the value at this point and its hierarchical position on the quad/octree. Then, an average process is performed for the coarsening, and a pass value is done for the refinement process in the computational space.

2.5 Numerical methods

The governing equations have been discretized using a finite-volume(FV) approach on a collocated unstructured grid arrangement according to [6], which automatically adapts to the AMR framework. Convective terms are discretized using TVD Superbee flux limiter scheme [6, 10], unless otherwise stated. Moreover, central difference scheme (CD) is also available for discretization. Diffusive terms are discretized employing CD scheme[6]. Surface tension force is taken into account using a continuos surface model[20], formulated for unstructured meshes by [6, 10]. A fractional step projection method is used for solving the pressure-velocity coupling [21, 10]:

$$\frac{\rho\mathbf{v}^* - \rho^n\mathbf{v}^n}{\Delta t} = \mathbf{C}^n + \mathbf{D}^n + \rho\mathbf{g} + \sigma\kappa\nabla_h(\phi) \qquad \mathbf{v}^{n+1} = \mathbf{v}^* - \frac{\Delta t}{\rho}\nabla_h(p^{n+1}) \tag{8}$$

where, $\mathbf{C} = -\nabla_h \cdot (\rho\mathbf{v}\mathbf{v})$, $\mathbf{D} = \nabla_h \cdot (\mu(\nabla_h\mathbf{v}) + (\nabla_h\mathbf{v})^T)$, $(\nabla_h\mathbf{v})^T$ is calculated by the least-squares method[6]. Combining the incompressible constraint with corrector step in Eq. 8, a Poisson equation for the pressure field is obtained, which is solved by means of a preconditioned conjugated gradient method:

$$\nabla_h \cdot \left(\frac{1}{\rho}\nabla_h(p^{n+1})\right) = \frac{1}{\Delta t}\nabla_h \cdot (\mathbf{v}^*) \tag{9}$$

Further technical details, verifications and validations of the numerical code in the framework of both CLS and VOF/LS methods have been reported in [6, 7, 8, 9, 10]. The

numerical algorithms explained in this work are implemented in a parallel C++/MPI code called TermoFluids.

3 NUMERICAL EXPERIMENTS

Test cases are presented to validate the present numerical methods in the context of single buoyancy driven motion bubbles. In the next sections, the verification and validation of the proposed AMR algorithm with CLS and VOF/LS are shown, in the context of 2D and 3D single bubbles. The dimensionless numbers controlling the rising of a quiescent bubble flows are the Eötvös number (Eo), Reynolds number (Re), Morton number (M) and the ratios of physical properties (density ratio η_ρ and viscosity ratio η_μ) defined as following

$$Eo = \frac{gd^2\Delta\rho}{\sigma} \quad M = \frac{g\mu_1^4\Delta\rho}{\rho_1^2\sigma^3} \quad Re = \frac{\rho_1 U_T d}{\mu_1} \quad \eta_\rho = \frac{\rho_1}{\rho_2} \quad \eta_\mu = \frac{\mu_1}{\mu_2} \tag{10}$$

where the subindex 1 refers to the continuous fluid phase, the subindex 2 refers to the lighter fluid in the bubble, the subindex d refers to the dispersed phase.

$U_T = \int_{\Omega_2} v_y \phi dV / \int_{\Omega_2} dV$ is the terminal velocity of the bubble, $\Delta\rho = \rho_1 - \rho_2$ specifies the density difference between the fluid phases. Furthermore, in order to get a quantitative measure of bubble shape, the sphericity is defined as $\zeta = \pi d^2 / \int_\Omega ||\nabla f|| dV$.

3.1 Two-dimensional rising bubble

Solutions are obtained on a computational domain of [-d_b,d_b];[0,4d_b], where the initial cylindrical bubble of diameter $d_b = 5.0$ is located at x=0, y=d_b (See Fig. 2). The boundary conditions at the top and bottom are non-slip conditions, and on the vertical walls, a free-slip boundary condition is applied. The fluid parameters are: $Eo = 10$, $Re = 35$, $\rho_1/\rho_2 = 10$, $\mu_1/\mu_2 = 10$, where the subscript 1 is used for the continuous fluid phase, Ω_1, while the subscript 2 is assigned to the lighter fluid in the bubble, Ω_2.

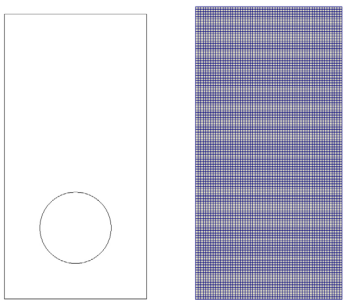

Figure 2: Illustration of the computational domain (left)Bubble initial position (right)computational base grid-number of control volumes 7k.

Present simulations are performed using AMR to ensure grid resolution on the interface

between fluids. Following the numerical studies carried out by [6], a minimum grid size was fixed on the interface with three levels of refinement for VOF/LS($h_{min} = d_b/240$) and three/four levels of refinement for CLS($h_{min} = d_b/240$ and $h_{min} = d_b/480$), to maximize the resolution of the bubble and reduce the overall number of control volumes for this case(total number of control volumes for three levels of refinement 9.3k aprox. and for four levels of refinement 37k aprox.). More refinement was achieved for CLS method because the interface is more wide compared to VOF/LS that has an interface thickness of one cell. The predicted bubble shapes on different times, defined as $t^* = tg^{1/2}d^{-1/2}$, with its AMR mesh are shown in Fig. 3.

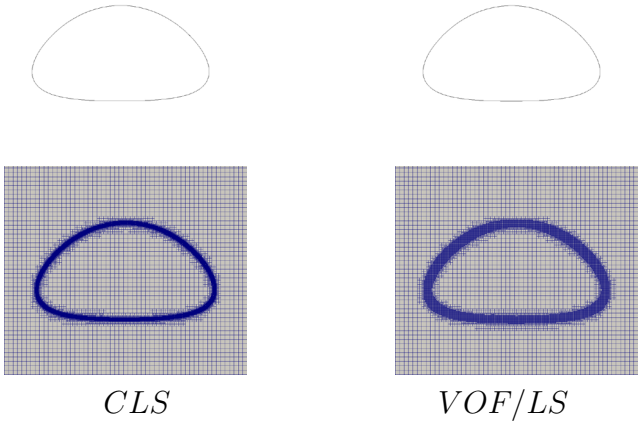

Figure 3: Example of a two dimensional rising bubble with CLS and VOF/LS at $t^* = 4.20$. Bubble shape with its computational grid.

For the sake of comparison, the benchmark quantities are defined as follows:

$$v_c = \frac{\int_{\Omega_2} \mathbf{v} \cdot \mathbf{e}_y dV}{\int_{\Omega_2} dV}, \qquad y_c = \frac{\int_{\Omega_2} \mathbf{x} \cdot \mathbf{e}_y dV}{\int_{\Omega_2} dV}, \qquad \zeta = \frac{\pi d_b^2}{\int_{\Omega} ||\nabla f(\mathbf{x}, t)|| dV}. \tag{11}$$

where v_c is the rise velocity, $\mathbf{e}_y$ is a unit vector parallel to the $y - axis$, y_c is the bubble centroid, ζ is the bubble circularity which takes the value 1 for a perfect circular bubble and values less than unity as the bubble is deformed.

Fig. 4 shows the position of the bubble, terminal Reynolds number, and circularity as a function of time. Our results compare well with the data published by [23, 24]. Both approaches show a correct representation of the dimple ellipsoidal bubble. Where the bubble being initially circular has a horizontal change, then the interfacial curvature gets smaller and, finally, tends to a certain limit value. This bubble deformation develops a slight dimple at the bottom but, at later times, eventually reaches a more stable ellipsoidal shape.

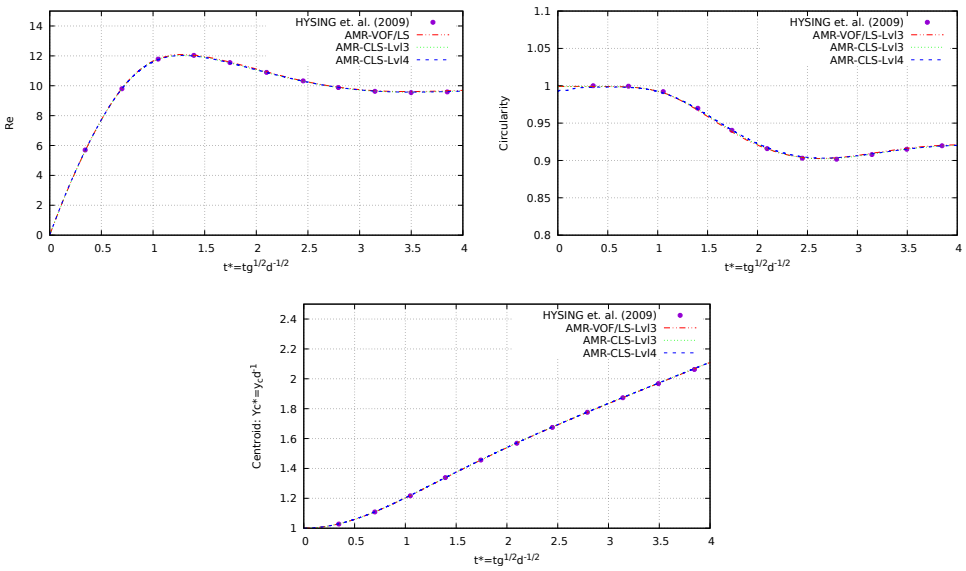

Figure 4: Two dimensional rising bubble results compared against[23]. (left top)Rise velocity (right top)Circularity (bottom)Bubble centroid

3.2 Three-dimensional buoyant bubbles

While the dynamics of a 2D single bubble is important for understanding the physical process of a rising bubble according to the dimensionless numbers, yet more useful information can be extracted from the analysis of a fully 3D single bubble. Experimental studies and correlations are usually invoked for the estimation of some macroscopic characteristics of the rising bubble. Rising bubble in ellipsoidal shape regime in an initially quiescent liquid is explored. The computational domain are $[0,8d_b];[0,16d_b];[0,8d_b]$, where the initial bubble of diameter $d_b = 2.5$ is located at x=0, y=$3d_b$ as it is shown in Fig. 5.

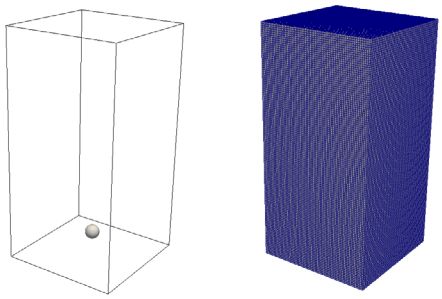

Figure 5: Illustration of the computational domain (left)Bubble initial position (right)computational base grid-number of control volumes 524k.

The fluid parameters are: $Eo = 116$, $Mo = 41.1$, $\rho_1/\rho_2 = 100$, $\mu_1/\mu_2 = 100$, No-

	[25]	[8]	[9]	Present AMR-CLS	Present AMR-VOF/LS
Number of cells		2.30E6	2.92E6	8.25E5	7.75E5
Re	7.16	6.94	7.02	6.79	6.76

Table 1: Present Re computations compared against experimental results from [25] and numerical results from [8, 9].

slip boundary condition is used at the top/bottom boundaries, and free-slip boundary condition is used at the lateral side of the domain. The mesh configurations follow an AMR strategy for 3D hexahedral elements. Following the numerical studies presented by [9], a minimum grid size was fixed on the interface ($h_{min} = d_b/64$), to maximize the resolution of the bubble and reduce the overall number of control volumes for this case (total number of control volumes 825k aprox.).

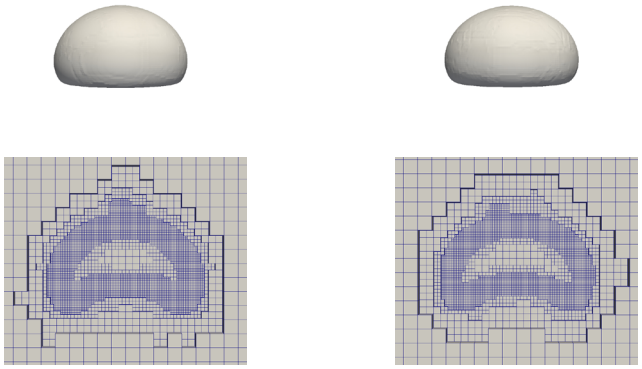

Figure 6: Example of a three dimensional rising bubble with CLS and VOF/LS at $t^* = 6.2$. Bubble shape with its computational grid.

A sequence of shapes for different times is presented in Fig. 6. Bubble start to rise due to buoyancy and starts to stretch tending to form a dimple at the bottom. This is produced due to the bubble tries to achieve a skirted shape but, finally reaches a dimple ellipsoidal shape, where it remains. The numerical prediction for terminal Reynolds number is compared with the numerical results reported by [8, 9] (See Table 1). A close agreement between CLS and VOF/LS results are obtained. Furthermore, CLS shows better mass conservation compared to VOF/LS (See Fig. 7). Here, the instantaneous mass is evaluated and compared with the initial mass, then the mass conservation error is calculated by $Mr = [M(t) - M(0)]/M(0)$ with $M(t) = \int_\Omega f dV$.

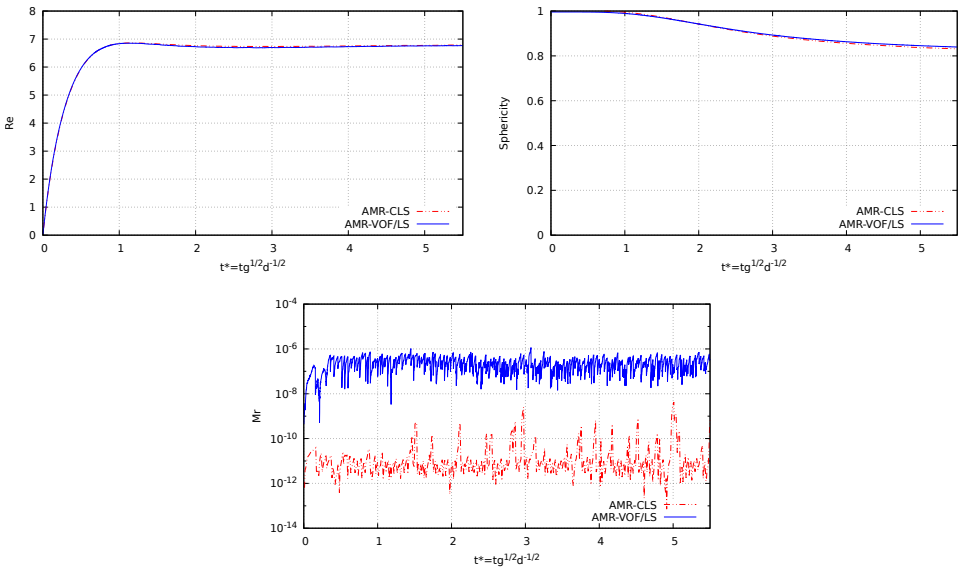

Figure 7: Three dimensional rising bubble results. (left top)Rise velocity (right top)Sphericity (bottom)Mass conservation error

4 CONCLUSIONS

- In this work, a comparative of CLS and VOF/LS for the simulation of incompressible two-phase flows using AMR technique was presented. Both methods were coupled with the Navier-Stokes equations discretized in a finite-volume scheme.

- The combination of the interface capturing methods and AMR technique results in an efficient algorithm that allows simulating complex two-phase flows with a reduction of computational resources in comparison with those used for fixed meshes.

- Present results are in good agreement with numerical and experimental results from the literature. As future work, this methodology will be extended to AMR for tetrahedral meshes, as well as, interfacial flows with heat and mass trasfer, phase change and variable surface tension[10].

5 ACKNOWLEDGMENTS

This work has been financially supported by the *Ministerio de Economía y Competitividad, Secretaría de Estado de Investigación, Desarrollo e Innovación (MINECO)*, Spain (ENE2015-70672-P), and by Termo Fluids S.L. Oscar Antepara acknowledges cofinancial support in form of a doctoral scholarship DI-14-06886 of the *MINECO* and 2015DI-68 of the *Secretaria d' Universitats i Recerca del Departament d'Economia i Coneixement de la Generalitat de Catalunya*, Spain. Néstor Balcázar acknowledges financial support of the *Programa Torres Quevedo, MINECO* (PTQ-14-07186), Spain.

REFERENCES

[1] Sussman, M., Smereka, P., Osher, S., A Level Set Approach for Computing Solutions to Incompressible Two-Phase Flow. *J. Comput. Phys* (1994) **144**:146–159.

[2] Sussman, M., Puckett, E.G., A Coupled Level Set and Volume-of-Fluid Method for Computing 3D and Axisymmetric Incompressible Two-Phase Flows. *J. Comput. Phys* (2000) **162**:301–337.

[3] Hirt, C., Nichols, B., Volume of fluid (VOF) method for the dynamics of free boundary. *J. Comput. Phys* (1981) **39**:201–225.

[4] Gueyffier, D., Li, J., Nadim, A., Scardovelli, R., Zaleski, S., Volume-of-fluid interface tracking with smoothed surface stress methods for three-dimensional flows. *J. Comput. Phys* (1999) **152**:423–456.

[5] Sun, D.L., Tao, J., W.Q., A coupled volume-of-fluid and level-set (VOSET) method for computing incompressible two-phase flows. *International Journal of Heat and Mass Transfer* (2010) **53**:645–655.

[6] Balcázar, N., Jofre, L., Lehmkhul, O., Castro, J., Rigola, J., A finite-volume/level-set method for simulating two-phase flows on unstructured grids. *International Journal of Multiphase Flow* (2014) **64**:55–72.

[7] Balcázar, N., Lemhkuhl, O., Rigola, J., Oliva, A., A multiple marker level-set method for simulation of deformable fluid particles. *International Journal of Multiphase Flow* (2015) **74**:125–142.

[8] Balcázar, N., Lemhkuhl, O., Jofre, L., Oliva, A., Level-set simulations of buoyancy-driven motion of single and multiple bubbles. *International Journal of Heat and Fluid Flow* (2015) **56**:91–107.

[9] Balcázar, N., Lemhkuhl, O., Jofre, L., Rigola, J., Oliva, A., A coupled volume-of-fluid/level-set method for simulation of two-phase flows on unstructured meshes. *Computers and Fluids* (2016) **124**:12–29.

[10] Balcázar, N., Rigola, J., Castro, J., Oliva, A., A level-set model for thermocapillary motion of deformable fluid particles. *International Journal of Heat and Fluid Flow* (2016), Part B,**62**:324–343.

[11] Olsson, E., Kreiss, G., A conservative level set method for two phase flow. *J. Comput. Phys.* (2005) **210**:225–246.

[12] Jofre, L., Lehmkuhl, O., Castro, J., Oliva, A., A 3-D Volume-of-Fluid advection method based on cell-vertex velocities. *Computers and Fluids* (2014) **94**:14–29.

[13] Antepara, O., Lehmkhul, O., Borrell, R., Chiva, J., Oliva, A., Parallel adaptive mesh refinement for large-eddy simulations of turbulent flows. *Computers and Fluids* (2015) **110**:48–61.

[14] Antepara, O., Borrell, R., Lehmkuhl, O., Rodrguez, I., Oliva, A., Parallel adaptive mesh refinement of turbulent flow around simplified car model using an immerse boundary method. *WCCM 2014, ECCM 2014 and ECFD 2014* (2014) 2603–2611.

[15] Antepara, O., Lehmkhul, O., Chiva, J., Borrell, R., Parallel adaptive mesh refinement simulation of the flow around a square cylinder at Re = 22000. *Procedia Engineering* (2013) **61**:246–250.

[16] Schillaci, E., Antepara, O., Lehmkuhl, O., Balcázar, N., Oliva, A., Effectiveness of adaptive mesh refinement strategies in the dns of multiphase flows. *Proceedings of International Symposium Turbulent Heat and Mass Transfer VIII* (2015).

[17] Pivello, M.R., Villar, M.M., Serfaty, R., Roma, A.M., Siveira-Neto, A., A fully adaptive front tracking method for the simulation of two phase flows. *International Journal of Multiphase Flow* (2014) **58**:72–82.

[18] Ceniceros, H.D., Nos, R.L., Roma, A.M., Three-dimensional, fully adaptive simulations of phase-field fluid models. *J. Comput. Phys.* (2010) **229**:6135–6155.

[19] Peskin, C.S., Numerical analysis of blood flow in the heart. *J. Comput. Phys.* (1977) **25**:220–252.

[20] Brackbill, J.U., Kothe, D.B., Zemach, C., A Continuum Method for Modeling Surface Tension. *J. Comput. Phys.* (1992) **100**:335–354.

[21] Chorin, A.J. Numerical solution of the Navier-Stokes equations. *Math. Comput.* (1968) **22**:745–762.

[22] Chang, Y.C., Hou, T.Y., Merriman, B., Osher, S., A level-set formulation of Eulerian interface capturing methods for incompressible two-phase flows. *J. Comput. Phys.* (1996) **124**:462–488.

[23] Hysing, S., Turet, S., Kuzmin, D., Parolini, N., Burman, E., Ganesan, S., Tobiska, L., Quantitative benchmark computations of two-dimensional bubble dynamics. *International Journal for Numerical Methods in Fluids* (2009) **60**:1259–1288.

[24] Hysing, S., Mixed element FEM level set method for numerical simulation of immiscible fluids. *J. Comput. Phys.* (2012) **231**:2449–2465.

[25] Bhaga, D., Weber, M.E., Bubbles in viscous liquids: shapes, wakes and velocities. *J. Fluid Mech.* (1981) **105**:61–85.